



Published in final edited form as:

*Leukemia*. 2024 May ; 38(5): 1143–1155. doi:10.1038/s41375-024-02218-6.

## STAT3 protects hematopoietic stem cells by preventing activation of a deleterious autocrine type-I interferon response

Bhakti Patel<sup>1</sup>, Yifan Zhou<sup>1</sup>, Rachel L. Babcock<sup>1,2</sup>, Feiyang Ma<sup>3,4</sup>, M. Anna Zal<sup>5</sup>, Dhiraj Kumar<sup>6</sup>, Yusra B. Medik<sup>1</sup>, Laura M. Kahn<sup>1,2</sup>, Josué E. Pineda<sup>1,2</sup>, Elizabeth M. Park<sup>1,7</sup>, Sarah M. Schneider<sup>1,2</sup>, Ximing Tang<sup>8</sup>, Maria Gabriela Raso<sup>8</sup>, Collene R. Jeter<sup>9</sup>, Tomasz Zal<sup>5</sup>, Karen Clise-Dwyer<sup>10</sup>, Khandan Keyomarsi<sup>11</sup>, Filippo G. Giancotti<sup>6</sup>, Simona Colla<sup>5</sup>, Stephanie S. Watowich<sup>1,2,12</sup>

<sup>1</sup>Department of Immunology, The University of Texas MD Anderson Cancer Center, Houston, TX, USA

<sup>2</sup>MD Anderson Cancer Center UTHealth Graduate School of Biomedical Sciences, Houston, TX, USA

<sup>3</sup>Molecular Biology Institute, University of California, Los Angeles, Los Angeles, CA, USA

<sup>4</sup>Division of Rheumatology, Department of Internal Medicine, Michigan Medicine, University of Michigan, Ann Arbor, MI, USA

<sup>5</sup>Department of Leukemia, The University of Texas MD Anderson Cancer Center, Houston, TX, USA

<sup>6</sup>Herbert Irving Cancer Center and Department of Genetics and Development, Columbia University, New York, NY, USA

<sup>7</sup>Department of Surgical Oncology, The University of Texas MD Anderson Cancer Center, Houston, TX, USA

<sup>8</sup>Department of Translational Molecular Pathology, The University of Texas MD Anderson Cancer Center, Houston, TX, USA

<sup>9</sup>Department of Epigenetics and Molecular Carcinogenesis, The University of Texas MD Anderson Cancer Center, Houston, TX, USA

<sup>10</sup>Department of Stem Cell Transplantation and Hematopoietic Biology and Malignancy, The University of Texas MD Anderson Cancer Center, Houston, TX, USA

**Correspondence:** Stephanie S. Watowich, PhD, Department of Immunology, Unit 902, The University of Texas MD Anderson Cancer Center, 1515 Holcombe Blvd., Houston, TX 77030, swatowic@mdanderson.org.

### Author Contributions

B.P. designed experiments, performed experiments, analyzed data, prepared data for presentation, and wrote the manuscript. Y.Z., R.L.B., Y.B.M., L.M.K., J.E.P., and E.M.P. assisted with sample collection and data analysis. D.K. assisted with scRNA-seq studies and analyzed data. F.M. curated scRNA-seq data, analyzed the results, and prepared data for presentation. M.A.Z., C.R.J. and T.Z. assisted with confocal microscopy and Imaris analysis. M.G.R. and X.T. performed pathology assessments. S.M.S. and K.C.-D. assisted with flow cytometry data analysis. K.K. provided advice and reviewed cell cycle data. F.G.G. provided advice on scRNA-seq data analyses. S.C. analyzed scRNA-seq data, performed validation, provided advice on data interpretation and presentation. S.S.W. conceptualized the study, designed experiments, procured funding, supervised the study, and wrote the manuscript.

Conflict of Interest Disclosures

Not applicable.

<sup>11</sup>Department of Experimental Radiation Oncology, The University of Texas MD Anderson Cancer Center, Houston, TX, USA

<sup>12</sup>Program for Innovative Microbiome and Translational Research (PRIME-TR), The University of Texas MD Anderson Cancer Center, Houston, TX, USA

## Abstract

Hematopoietic stem and progenitor cells (HSPCs) maintain blood-forming and immune activity, yet intrinsic regulators of HSPCs remain elusive. STAT3 function in HSPCs has been difficult to dissect as *Stat3* deficiency in the hematopoietic compartment induces systemic inflammation, which can impact HSPC activity. Here, we developed mixed bone marrow (BM) chimeric mice with inducible *Stat3* deletion in 20% of the hematopoietic compartment to avoid systemic inflammation. *Stat3*-deficient HSPCs were significantly impaired in reconstitution ability following primary or secondary bone marrow transplantation, indicating hematopoietic stem cell (HSC) defects. Single-cell RNA sequencing of Lin<sup>-</sup>cKit<sup>+</sup>Sca1<sup>+</sup> BM cells (LSKs) revealed aberrant activation of cell cycle, p53, and interferon (IFN) pathways in *Stat3*-deficient HSPCs. *Stat3*-deficient LSKs accumulated  $\gamma$ H2AX and showed increased expression of DNA sensors and type-I IFN (IFN-I), while treatment with A151-ODN inhibited expression of IFN-I and IFN-responsive genes. Further, the blockade of IFN-I receptor signaling suppressed aberrant cell cycling, STAT1 activation, and nuclear p53 accumulation. Collectively, our results show that STAT3 inhibits a deleterious autocrine IFN response in HSCs to maintain long-term HSC function. These data signify the importance of ensuring therapeutic STAT3 inhibitors are targeted specifically to diseased cells to avoid off-target loss of healthy HSPCs.

## Keywords

hematopoietic stem cell; STAT3; IFN signaling; DNA damage; p53

## Introduction

In homeostatic conditions, the replenishment of peripheral immune cells is sustained by relatively quiescent hematopoietic stem cells (HSCs), which undergo differentiation to generate mature blood lineages or self-renew to maintain the stem cell pool [1, 2]. The hematopoietic system is dynamic and can adapt to physiological stress by increasing blood cell production [3]. Following the resolution of a transient demand such as bacterial infection, HSCs reestablish homeostasis and return to a largely dormant state [2]. However, dysregulation of these mechanisms can result in persistent HSC activation and dysfunction, subsequently increasing the propensity for bone marrow (BM) failure, preleukemic transformation, or inflammatory disorders [4, 5]. Moreover, acquired mutations in HSCs can lead to clonal hematopoiesis, increased risk of blood cancers, and higher mortality in atherosclerotic cardiovascular disease [6]. Identifying the intrinsic mechanisms that regulate HSCs is crucial to improving our understanding of hematopoiesis and devising therapeutic interventions for disorders associated with HSC dysfunction [7, 8].

Chronic inflammatory signals from cytokines, interferons (IFNs), infectious microbes, or Toll-like receptor (TLR) agonists can trigger the loss of HSC quiescence as well as HSC exhaustion, age-associated hematopoietic deregulation (inflammaging), and the impairment of long-term HSC (LT-HSC) activity [7, 9, 10, 11, 12]. Excessive exposure to these factors can deregulate HSCs directly or through changes in key components of the HSC niche [12, 13]. For instance, sustained signaling by exogenous IFN- $\alpha$  or IFN- $\gamma$  leads to loss of HSC function and myeloid-skewed hematopoiesis [12, 14, 15, 16]. Impaired HSC self-renewal due to persistent IFN exposure has important clinical implications, including hematopoietic dysfunction in patients with aplastic anemia, thrombocytopenia, or individuals undergoing CAR-T immunotherapy [15, 16, 17]. Furthermore, deregulation of intrinsic anti-inflammatory factors in HSCs, such as miR-146a or ADAR1, causes excessive activation of inflammatory or IFN signaling cascades, leading to HSC damage and BM failure [18, 19, 20, 21].

The signal transducer and activator of transcription 3 (STAT3) is a cytokine-responsive transcriptional regulator involved in numerous immune and hematopoietic functions. STAT3 has a significant anti-inflammatory role in mature myeloid cells, dendritic cells (DCs), and non-immune cell populations [22, 23]. This function is mediated in a cell type-specific manner by restraint of NF- $\kappa$ B-responsive pro-inflammatory cytokine production or suppression of IFN signaling [24, 25]. Previous studies implicated STAT3 in HSC regulation, yet these were confounded by the systemic inflammation that accompanies hematopoietic *Stat3* deletion or by *Stat3*-deficiency in BM and non-hematopoietic BM niche cells [22, 26, 27, 28, 29]. Thus, novel approaches are needed to dissect the physiological role of STAT3 in HSCs.

Here, we addressed the gap in understanding STAT3's intrinsic function in HSCs using competitive mixed BM chimeric mice with conditional *Stat3* deletion in ~20% of the hematopoietic compartment. With this approach, wild-type blood cells were the major peripheral population, enabling study of *Stat3*-deficient HSPCs without systemic inflammation. Our results reveal STAT3 has an essential role in HSPCs to inhibit excessive proliferation, DNA damage, autocrine IFN-I signaling, and p53 activation. This function is required to preserve HSC amounts and long-term hematopoietic activity.

## Methods

### Mice

CreER *Stat3<sup>f/f</sup>* mice were generated as described [29]. Age- and sex-matched CreER Gt(ROSA)26Sor<sup>tm1(creERT2)Tyj</sup> animals (The Jackson Laboratory, Bar Harbor, ME) were used as controls unless mentioned otherwise [29]. Congenic B6SJL-Ptprca Pepcb/boyj (CD45.1<sup>+</sup>) mice (The Jackson Laboratory) were used as BM transplant recipients [29]. CD45.1<sup>+</sup>CD45.2<sup>+</sup> mice were generated by crossing congenic CD45.1<sup>+</sup> mice with C57BL/6 (CD45.2<sup>+</sup>) mice. Animals were maintained in a specific pathogen-free facility at MD Anderson. All experimental procedures were performed in accordance with protocols approved by MD Anderson's Institutional Animal Care and Use Committee.

## Competitive BM transplantation assays

BM cells were flushed from the femurs and tibias of donor mice into sterile DMEM containing 1% heat-inactivated fetal bovine serum. For primary mixed BM chimeras, BM cells from CreER or CreER *Stat3<sup>fl/fl</sup>* (CD45.2<sup>+</sup>) mice were mixed with CD45.1<sup>+</sup>CD45.2<sup>+</sup> wildtype (WT) competitor BM cells at a 1:4 ratio prior to transplantation. Eight-week-old congenic recipient CD45.1<sup>+</sup> mice were lethally-irradiated (920 rad) and intravenously injected with  $2 \times 10^6$  mixed BM cells. To evaluate reconstitution efficiency, peripheral blood (PB) lineages were measured at 4-week intervals.

For conditional *Stat3* deletion, mixed BM chimeric mice were injected intraperitoneally with 2 mg of tamoxifen every other day for 1 week (3 treatments total), starting 8 weeks after BM transplantation. For secondary transplantations,  $2 \times 10^6$  BM cells were isolated from mixed BM chimeric mice 8 weeks after tamoxifen treatment and transferred to lethally-irradiated (920 rad) secondary CD45.1<sup>+</sup> recipients. Hematopoietic activity was assessed by measuring PB chimerism at 4-week intervals after tamoxifen treatment (primary transplants) or every 4 weeks after secondary transplantation.

## Single-cell RNA sequencing (scRNA-seq)

For these assays, we used mice injected with a 1:1 ratio of CD45.2<sup>+</sup> test (CreER or CreER *Stat3<sup>fl/fl</sup>*) and CD45.1<sup>+</sup>CD45.2<sup>+</sup> WT competitor cells to ensure sufficient Lin<sup>-</sup>ckit<sup>+</sup>Sca1<sup>+</sup> cells (LSKs) for sequencing. We used fluorescence-activated cell sorting (FACS) to purify donor-derived test (CD45.2<sup>+</sup>) and competitor (CD45.1<sup>+</sup>CD45.2<sup>+</sup>) LSKs from mixed BM chimeric mice with CreER or CreER *Stat3<sup>fl/fl</sup>* cells (n = 15 mice per experimental group) 8 weeks after tamoxifen treatment. Single-cell suspensions (1000 cells/ $\mu$ L) were submitted to MD Anderson's Advanced Technology Genomics Core Facility. Cell viability was assessed, and samples were loaded onto a Chromium Single Cell Chip (10X Genomics, Pleasanton, CA) and processed for lysing and barcoding at a target capture rate of 10,000 single cells per sample. Barcoded libraries were pooled and sequenced using a NovaSeq 6000 100-cycle flow cell (Illumina, San Diego, CA) to an average depth of 100,000 reads per cell.

## Statistical analysis

Statistical analysis was performed using Prism (version 8.0, GraphPad, San Diego, CA). All experiments were performed independently at least two times. Significant differences were determined using a two-tailed unpaired Student *t*-test or one- or two-way ANOVA with the Sidak or Tukey multiple comparison test. The exact sample size for each experiment is provided in the figure legends. Data were normally distributed and represented as the mean  $\pm$  SEM. A p value of <0.05 was used to indicate statistical significance.

A detailed description of the methods used in the study is provided in the Supplementary Data.

## Results

### STAT3 controls hematopoiesis in the absence of systemic inflammation

To investigate STAT3's role in hematopoiesis without concurrent systemic inflammation, we established mixed BM chimeric mice with conditional *Stat3* deletion in ~20% of the hematopoietic compartment (Fig. 1A). This allowed us to track CD45.2<sup>+</sup> CreER *Stat3*<sup>fl/fl</sup> (*Stat3*-deficient) or CreER (*Stat3*-sufficient control) cells and CD45.1<sup>+</sup>CD45.2<sup>+</sup> wild-type (WT) competitors in the same background. After confirming engraftment, we treated mice with tamoxifen to induce *Stat3* deletion (Fig. 1A). *Stat3* was effectively depleted in CD45.2<sup>+</sup> BM cells from CreER *Stat3*<sup>fl/fl</sup> mice, yet negligible differences were found in circulating cytokines and chemokines, or colon histology, compared to *Stat3*-sufficient mice (Fig. 1B–D; Supplementary Table 1–3). Furthermore, proinflammatory cytokine expression was similar between *Stat3*-sufficient and -deficient total BM cells or LSKs, although *Stat3*-deficient granulocyte-monocyte progenitors (GMPs) had a modest increase in *Il1b* expression (Supplementary Fig. 1A–C). These data demonstrate that the mixed BM chimeric mice enable the evaluation of STAT3's function in the absence of systemic inflammation or substantial inflammatory cytokine production from BM cells.

The ability of *Stat3*-deficient HSPCs to generate PB was significantly impaired 4 weeks ( $P < 0.001$ ) and 8 weeks ( $P < 0.0001$ ) after *Stat3* deletion, as shown by the decreased number of circulating CD45.2<sup>+</sup> cells (Fig. 1E, left panel). This associated with an increased number of WT competitor cells (Fig. 1E, right panel), suggesting that *Stat3*-deficient HSPCs have a competitive disadvantage. Furthermore, CD45.2<sup>+</sup> myeloid cells, neutrophils, monocytes, and T and B cells in PB were significantly depleted 8 weeks after *Stat3* deletion, whereas circulating WT competitor populations had increased chimerism (Fig. 1F; Supplementary Fig. 2A–C). We also observed a significant depletion of CD45.2<sup>+</sup> immune subsets in spleen and colonic lamina propria of mice with *Stat3*-deficient BM, while WT competitor populations were increased in spleens of mice with *Stat3* deletion (Fig. 1G–I; Supplementary Fig. 2D–G). Together, our results indicate that STAT3 is crucial for sustaining the effective production of mature hematopoietic cells in the absence of systemic inflammation.

### STAT3 controls progenitor and differentiated BM subsets

To further understand STAT3 function, we evaluated BM populations in chimeric mice 8 weeks after *Stat3* deletion. Total CD45.2<sup>+</sup> cells, as well as CD45.2<sup>+</sup> myeloid (CD11b<sup>+</sup>) cells, Gr1<sup>+</sup> neutrophils, and Lin<sup>−</sup> cells were significantly reduced in chimeric mice with *Stat3*-deficient BM, whereas WT competitor populations were increased (Fig. 2A–C). By contrast, CD45.2<sup>+</sup> LSKs, LT-HSCs, myeloid-biased multipotent progenitors (MPP-Mye), lymphoid-biased MPPs (MPP-Ly), and committed progenitor subset amounts were maintained up to 8 weeks after *Stat3* deletion (Fig. 2D; Supplementary Fig. 3A–C). These results indicate that removal of STAT3 does not rapidly affect maintenance of long-lived HSPCs, whereas STAT3 is required to sustain Lin<sup>−</sup> cells and differentiated lineages in the BM.

We observed a slight increase in CD45.2<sup>+</sup> progenitor populations in CreER BM chimeras after tamoxifen treatment, along with reduction of WT competitor HSPCs (Fig. 2D);

Supplementary Fig. 3C, D), suggesting modest effects of tamoxifen on *Stat3*-sufficient HSPCs. Thus, we treated WT C57Bl/6J and CreER mice with tamoxifen and assessed PB subsets and BM progenitors 4 weeks later (Supplementary Fig. 4A). WT mice treated with vehicle for <24 hours (i.e., at 0 weeks) served as the control group. We observed a modest reduction in PB neutrophils in vehicle- and tamoxifen-treated CreER mice, as well as decreased monocytes in vehicle-treated CreER mice by 4 weeks. T cells were reduced in WT mice immediately following (0 week) and 4 weeks after tamoxifen treatment; however, tamoxifen treatment and CreER activation did not affect the proportion of total PB CD45.2<sup>+</sup>, myeloid, or B cells considerably (Supplementary Fig. 4B, C). By contrast, compared with WT controls at 0 weeks, CreER mice showed increases in the absolute numbers of BM LSKs, MPP-Mye, and common myeloid progenitors (CMP) 4 weeks after vehicle or tamoxifen treatment, while LT-HSCs increased with tamoxifen after 4 weeks (Supplementary Fig. 4D). These data suggest that CreER, tamoxifen, and tamoxifen-mediated activation of CreER modestly affect BM populations. Additionally, tamoxifen appeared to provide a mild protection from apoptosis in CreER LSKs and HSCs, however, it had no discernable influence on cell cycle progression (Supplementary Fig. 4E, F), suggesting that the response of HSPCs to CreER activation is transient.

### HSCs require STAT3 for long-term hematopoietic function

To formally evaluate the function of *Stat3*-deficient HSCs, we performed secondary BM transplantation assays. BM cells were isolated from chimeric CreER or CreER *Stat3*<sup>fl/fl</sup> mice 8 weeks after tamoxifen treatment and used to reconstitute lethally-irradiated CD45.1<sup>+</sup> congenic mice (Fig. 3A). Donor-derived *Stat3*-deficient cells were significantly impaired in their ability to sustain hematopoiesis, as demonstrated by loss of PB CD45.2<sup>+</sup> cells, while circulating CD45.1<sup>+</sup>CD45.2<sup>+</sup> WT competitor cells were significantly increased in mice that received *Stat3*-deficient BM (Fig. 3B, C; Supplementary Fig. 5A). Moreover, *Stat3*-deficient BM failed to reconstitute all BM progenitor populations analyzed including LT-HSCs (Fig. 3D–H; Supplementary Fig. 5B, C). Taken together, these results reveal that STAT3 is required to maintain hematopoiesis, BM HSPC numbers, and LT-HSC function.

### STAT3-mediated transcriptional responses in HSPCs

To elucidate the impact of *Stat3*-deficiency in HSPCs, we performed scRNA-seq using LSKs purified from BM chimeric mice: CD45.2<sup>+</sup> CreER (*Stat3*-sufficient) LSKs and WT CD45.1<sup>+</sup>CD45.2<sup>+</sup> LSK competitors from CreER BM chimeric mice, and CD45.2<sup>+</sup> CreER *Stat3*<sup>fl/fl</sup> (*Stat3*-deficient) LSKs and WT CD45.1<sup>+</sup>CD45.2<sup>+</sup> LSK competitors from CreER *Stat3*<sup>fl/fl</sup> BM chimeric mice. We confirmed the absence of systemic inflammation in BM recipient mice used for LSK isolation (Fig. 4A; Supplementary Fig. 5D, E).

Analysis of the integrated LSK compartment from all experimental groups by Uniform Manifold Approximation and Projection (UMAP) for dimension reduction revealed 12 distinct transcriptional states (Fig. 4B). Individual clusters were defined by enriched expression of stem cell- and lineage-specific genes, revealing HSC- and MPP-like subpopulations as well as subpopulations defined by the expression of myeloid-, megakaryocyte/erythroid-, or lymphoid-specific genes (Fig. 4C; Supplementary Fig. 5F). Cells from all experimental groups were detected in each transcriptionally-defined cluster.

However, *Stat3*-deficient LSKs were more abundant in myeloid-biased (clusters 6 and 9) and megakaryocyte/erythroid (clusters 8 and 10) clusters, and less abundant in lymphoid (cluster 4) and cycling progenitor (clusters 1 and 5) clusters (Fig. 4D, E). While *Stat3*-deficient and -sufficient HSCs and MPPs (clusters 3 and 2, respectively) were found in similar abundance, *Stat3*-deficient populations had increased expression of genes associated with myeloid (*Mpo*, *Elane*, *S100a8*, and *S100a9*) and megakaryocyte/erythroid (*Pf4*) lineages, and decreased expression of genes associated with lymphoid lineages (*Ighm* and *Jchain*) (Fig. 4F; Supplementary Fig. 5G). These results suggest that STAT3 controls HSPC proliferation and suppresses the overproduction of early myeloid and megakaryocyte progenitors by restraining myeloid- and megakaryocyte-biased gene expression in multipotent BM progenitors.

To identify dysregulated transcriptional responses in *Stat3*-deficient HSPCs, we performed pathway enrichment analysis of our scRNA-seq data. Differential expression analysis comparing *Stat3*-deficient and -sufficient cluster 3 (HSCs) or cluster 2 (MPPs) revealed augmentation of transcriptional pathways related to cellular proliferation, signaling, and stress responses in *Stat3*-deficient HSCs and MPPs (Fig. 5A, B). Consistently, genes associated with cell cycle regulation and G1-S transition (e.g., *Cdk11b*, *Hp1bp3*, *Skp1a*) were upregulated in *Stat3*-deficient HSCs and MPPs (Fig. 5C; Supplementary Fig. 6A). We also observed increased expression of genes associated with DNA damage, cellular stress responses, and apoptosis (e.g., *H2afx*, *Tip53/p53*); p53 stabilization (*Xaf1*, *Rock1*, *Brd7*, *Kdm2a*); and p53-regulated genes (*Itih5*, *Gpx1*, *Mxd4*, *Fos*, *Sfr1*, *Tap1*) in *Stat3*-deficient HSCs and MPPs (Fig. 5D, E; Supplementary Fig. 6B–D). These findings suggest that *Stat3*-deficient HSCs and MPPs have an aberrant cell cycle and activation of the p53 response.

### STAT3 prevents excessive proliferation and p53 activation in HSPCs

To investigate whether STAT3 regulates HSPC proliferation, we examined the cell cycle status of LSKs in vitro. We observed a significant increase in the proportion of *Stat3*-deficient LSKs in the S/G2/M cell cycle phases, along with a decrease in G0/G1, indicating that acute STAT3 depletion promotes LSK cell cycle progression (Fig. 5F). Consistent with this observation, *Stat3*-deficient HSCs and MPPs were enriched for cell cycle-related transcriptional pathways (Fig. 5A, B).

Aberrant proliferation and replicative stress can lead to DNA damage in HSCs and early progenitors [30, 31, 32]. Thus, we quantified  $\gamma$ H2AX foci in cells purified from BM chimeric mice at various times following *Stat3* deletion (Supplementary Fig. 7A). *Stat3*-deficient LSKs showed significant increases in  $\gamma$ H2AX foci, particularly by 12 weeks after *Stat3* deletion in vivo (Fig. 5G; Supplementary Fig. 7B). In addition, we confirmed increased  $\gamma$ H2AX levels in *Stat3*-deficient LSKs in vitro (Fig. 5H). These results are consistent with the enhanced *H2afx* expression observed in *Stat3*-deficient HSCs and MPPs (Fig. 5D). WT competitor LSKs from *Stat3*-deficient BM chimeric mice showed a slight increase in  $\gamma$ H2AX foci at early time points (Fig. 5G), suggesting their compensatory proliferation after *Stat3* deletion. In addition, we found the DNA damage repair transcriptional pathway was enriched in *Stat3*-sufficient HSCs compared with WT competitors in the same background. This transcriptional response was not significantly

enriched in *Stat3*-deficient LSKs (Supplementary Fig. 7C, D), supporting the concept that STAT3 is required for an effective DNA damage response. Collectively, our results indicate that STAT3 depletion leads to increased proliferation and accumulation of DNA damage in HSPCs.

DNA damage from cell cycle deregulation or excessive proliferation is normally repaired in p53-intact cells by p53-mediated DNA damage response pathways [33, 34]. We found enrichment of the p53 pathway as well as p53 regulators and target genes in *Stat3*-deficient HSCs and MPPs (Fig. 5E; Supplementary Fig. 6B, C). Using confocal microscopy and immunofluorescence with purified LSKs, we observed significant increases in p53 nuclear localization in *Stat3*-deficient LSKs, indicating p53 stabilization and activation (Fig. 5I, J). By contrast, we did not detect significant changes in the expression of the cell cycle arrest factor p21, DNA damage-associated Rad51, or apoptosis-regulator Mcl1 in *Stat3*-deficient LSKs (Fig. 5I, J; Supplementary Fig. 7E, F). Thus, our results show STAT3 is required to prevent p53 activation in HSPCs, and further suggest that aberrant proliferation of *Stat3*-deficient HSPCs results in unrepaired DNA damage and p53 activation in vivo.

### **Cell-intrinsic IFN-I signaling leads to excessive proliferation and p53 activation in *Stat3*-deficient HSPCs**

Defects in the DNA damage response and repair system, as well as aberrant activation or mutations in genes associated with DNA-sensing pathways can induce the IFN response, while IFN-Is and type-II IFN (IFN- $\gamma$ ; IFN-II) stimulate HSPC proliferation [14, 16, 35, 36, 37]. We observed significant enrichment of the IFN- $\alpha$  and IFN- $\gamma$  transcriptional pathways in *Stat3*-deficient HSCs and MPPs, respectively (Fig. 5A, B). IFN-stimulated genes and IFN-responsive transcriptional regulators were also upregulated in *Stat3*-deficient HSCs and MPPs, while *Stat3* was depleted as expected (Fig. 6A, B; Supplementary Fig. 8A, B). We confirmed *Stat3*-deficient BM cells had increased expression of IFN-response genes compared with *Stat3*-sufficient BM cells or WT competitors (Fig. 6C). To evaluate whether DNA sensing was involved in mediating IFN-I signaling in *Stat3*-deficient HSPCs, we treated LSKs with A151-ODN, an oligonucleotide inhibitor of murine Ifi200 family members involved in DNA sensing [38]. A151-ODN treatment attenuated the increased expression of IFN-I (*Ifnb*), IFN signaling genes (*Irf7*, *Stat1*), and DNA sensors (*Ifi203*, *Ifi204*) in *Stat3*-deficient LSKs, without affecting expression of these genes in *Stat3*-sufficient (CreER) LSKs. By contrast, we did not detect enrichment of *Trem173* or other genes associated with cGAS-STING signaling (Fig. 6D; Supplementary Fig. 8C). These data show that STAT3 prevents activation of IFN-associated transcriptional responses in HSCs and MPPs, which are stimulated in *Stat3*-deficient cells through a DNA sensing pathway.

In addition to promoting HSPC proliferation, IFN-Is can induce p53 expression and activation, while IFN-stimulated genes can trigger p53 stabilization [15, 39, 40, 41]. Thus, we evaluated the effects of blocking IFNAR1, a component of the IFN-I receptor, on *Stat3*-deficient LSK responses. Anti-IFNAR1 treatment significantly impaired p53 activation and reduced excessive proliferation of *Stat3*-deficient LSKs (Fig. 6E–H). Consistently, we observed increased STAT1 tyrosine phosphorylation (Y701) in *Stat3*-deficient LSKs, which was significantly repressed by IFNAR1 blockade (Fig. 6I). These data demonstrate



that IFN-I autocrine signaling induces proliferation and p53 activation in *Stat3*-deficient LSKs. Together, our results show that STAT3 restrains an autocrine IFN response that has deleterious consequences in HSPCs and thereby serves as a critical protective factor for the LT-HSC population.

## Discussion

A significant knowledge gap has centered on the role for STAT3 in HSCs due to confounding effects of previous experimental models, including the systemic inflammation that accompanies hematopoietic-intrinsic *Stat3* deletion [22, 26, 27, 28, 29]. To address this, we generated mice with CreER-mediated deletion of *Stat3* in ~20% of the BM, which avoided systemic inflammation. This strategy also allowed evaluation of *Stat3*-deficient HSPCs and *Stat3*-sufficient WT competitor cells in the same environment, and enabled comparisons with prior work [29]. Our results revealed an unrecognized function for STAT3 in restraining DNA damage and DNA sensor-mediated induction of autocrine IFN-I signaling, which drives excessive proliferation and p53 activation in HSPCs. STAT3 protective function is required to maintain LT-HSCs and the effective production of mature immune lineages from the HSC pool in the absence of systemic inflammation.

Prior work illuminated both promoting and inhibiting roles for STAT3 in cell proliferation. For example, STAT3 governs G1/S transition and accelerates cell cycle progression in specific immune progenitor populations or non-immune cells, particularly in response to cytokines [42, 43], while STAT3 suppresses proliferation of Jak2V617F-expressing LSKs [44]. We found that acute loss of STAT3 triggered enhanced LSK proliferation in vitro, while absolute numbers of HSCs and progenitor subsets were maintained for up to 8 weeks in primary BM chimeric mice following *Stat3* deletion in vivo. By contrast, we found fewer LSKs within proliferative subsets 8 weeks after *Stat3* deletion, as judged by our scRNA-seq data, and *Stat3*-deficient LT-HSCs and progenitors were significantly depleted after secondary BM transplantation. Excessive proliferation and replicative stress causes HSC exhaustion and loss [30, 31, 45]. Taken together, these data suggest long-lived progenitors can remain viable after *Stat3* deletion but accrue damage over time as a consequence of excessive proliferation and are eventually removed from the LT-HSC pool.

Persistent HSC proliferation and cell cycle deregulation can damage nuclear DNA [30, 31]. *Stat3*-deficient LSKs accumulate DNA damage and demonstrate elevated nuclear amounts of p53, a key DNA damage and cellular stress response factor. Consistently, *Stat3*-deficient HSCs and MPPs have increased *Trp53* (p53) gene expression and a p53-associated transcriptional signature. Previous studies implicate p53 in regulating HSC quiescence and self-renewal by activating apoptosis or cell cycle arrest under normal and stress conditions [34, 46, 47]. Gain-of-function or loss-of-function *Trp53* mutations are associated with several hematological malignancies [47, 48]. Furthermore, an overactive p53 response is induced in patients with BM failure syndromes associated with unresolved cellular stress, DNA damage, or telomere attrition, which leads to HSC exhaustion [49, 50, 51]. In our work, *Stat3*-deficient HSPCs did not show evidence of apoptosis or cell cycle arrest, suggesting alternative mechanisms for LT-HSC loss, such as exhaustion from unrestrained proliferation or p53 overactivation.

*Stat3*-deficient LSKs also demonstrated enhanced IFN transcriptional responses, increased accumulation of myeloid and megakaryocyte/erythroid subpopulations at the expense of lymphoid subpopulations, and elevated expression of myeloid- and megakaryocyte-lineage genes. Nonetheless, we did not detect enhanced myelopoiesis in our competitive BM chimeric mice with *Stat3*-deficiency. In fact, myeloid subsets were rapidly depleted upon *Stat3* deletion, in agreement with previous studies that showed STAT3 has key roles in stimulating proliferation of committed myeloid and immune progenitors [43, 52]. Thus, while loss of STAT3 affects lineage-related gene expression in HSPCs, this does not lead to lineage-biased hematopoiesis due to roles for STAT3 in supporting progenitor subsets at later developmental stages. By contrast, in the context of systemic inflammation, *Stat3*-deficient HSPCs generate myeloid-biased hematopoiesis [29]. These results suggest that STAT3-independent mechanisms govern excessive production of *Stat3*-deficient myeloid cells during inflammation, consistent with prior work showing that pathways such as IFN-STAT1 or interleukin-1 signaling induce myeloid-biased hematopoiesis [53, 54].

IFN-Is and IFN-II, provided exogenously or elicited with infection, have direct and indirect effects on hematopoiesis [12, 13], including promotion of biased differentiation towards myeloid and megakaryocyte lineages [14, 55, 56], enhanced HSC proliferation, and activation of p53-mediated apoptosis [12, 15]. IFN-I effects on hematopoiesis are mediated via the IFN-I receptor IFNAR and its downstream signal transducer, STAT1 [12, 15]. Furthermore, cell-intrinsic activation of IFN-I signaling increases megakaryocyte-skewed differentiation of telomere-dysfunctional HSCs or JAK2V617F<sup>+</sup> HSCs [55, 57]. Recent studies have elucidated mechanisms of cell-intrinsic IFN-I activation via cytosolic dsDNA sensors [58]. We found increased expression of genes in the *Iff200* family of DNA sensors in *Stat3*-deficient HSPCs. In addition, A151-ODN, which inhibits the function of *Iff200* members, suppressed elevated expression of IFN-I and IFN-responsive genes in *Stat3*-deficient LSKs. This indicates roles for DNA sensing in IFN-I production and autocrine IFN-I signaling in *Stat3*-deficient HSPCs. IFNAR1 blockade restrained the proliferation of *Stat3*-deficient LSKs, as well as the activation of STAT1 and p53 in *Stat3*-deficient LSKs. Together, these results suggest that acute STAT3 loss leads to enhanced HSPC proliferation, resulting in DNA damage and activation of DNA sensors, and subsequent induction of cell-intrinsic IFN-I production and autocrine IFNAR signaling, which reinforces unrestrained proliferation and p53 activation. Thus, our findings suggest that activation of autocrine IFN-I signaling in *Stat3*-deficient HSPCs leads to the eventual loss of LT-HSCs in vivo.

Collectively our results reveal that STAT3 is essential to protect HSCs in absence of systemic inflammation. Caveats to our study include potential effects of CreER activation and tamoxifen, which we and others have found to modestly affect HSPCs [59, 60]. Furthermore, although we did not detect inflammatory cytokine production from *Stat3*-deficient BM subsets, with the exception of IFN-Is, we cannot completely exclude potential effects of microenvironmental inflammatory signals in our model. Nonetheless, our findings provide evidence of STAT3-mediated intrinsic mechanisms that preserve the function of normal HSPCs, which may facilitate the design of novel approaches involving STAT3 inhibition to remove damaged, leukemic, or diseased HSPCs without affecting healthy LT-HSCs. Overall, a full understanding of STAT3 activity in HSCs is needed to improve the therapeutic response of STAT3 inhibitors and prevent their unwanted off-target effects.

## Supplementary Material

Refer to Web version on PubMed Central for supplementary material.

## Acknowledgements

We thank Joseph Munch for his review and edits to this manuscript. This work was supported by grants from the Cancer Prevention and Research Institute of Texas (CPRIT) (Research Training award RP170067, R.L.B.) (Research Training awards RP170067 and RP210028, L.M.K. and E.M.P.), the National Institutes of Health (NIH) (F32 CA271513, E.M.P.; R35 CA197566, F.G.G. and D.K.; R01AI133822 and R56AI109294-06, S.S.W.). S.C. is a Scholar of the Leukemia and Lymphoma Society. This work used MD Anderson's Advanced Technology Genomics Core (supported by NIH 1S10OD024977-01 and NCI P30CA0166722), Research Histology Core Laboratory (supported by NCI P30CA0166722), Advanced Microscopy Core (supported by NIH S10RR029552), and Advanced Cytometry & Sorting Facility (supported by NCI P30CA0166722).

## Data and Materials availability

All data needed to evaluate the conclusions in the paper are present in the paper and/or the Supplementary Materials. The scRNA-seq data have been submitted to the NCBI GEO repository and are accessible through accession number (**GSE220466**).

## References

- Orkin SH, Zon LI. Hematopoiesis: an evolving paradigm for stem cell biology. *Cell*. 2008;132(4):631–44. [PubMed: 18295580]
- Wilson A, Laurenti E, Oser G, van der Wath RC, Blanco-Bose W, Jaworski M, et al. Hematopoietic stem cells reversibly switch from dormancy to self-renewal during homeostasis and repair. *Cell*. 2008;135(6):1118–29. [PubMed: 19062086]
- Zhao JL, Baltimore D. Regulation of stress-induced hematopoiesis. *Curr Opin Hematol*. 2015;22(4):286. [PubMed: 26049748]
- Yamashita M, Dellorusso PV, Olson OC, Passegué E. Dysregulated haematopoietic stem cell behaviour in myeloid leukaemogenesis. *Nat Rev Cancer*. 2020;20(7):365–82. [PubMed: 32415283]
- Zon LI. Intrinsic and extrinsic control of haematopoietic stem-cell self-renewal. *Nature*. 2008;453(7193):306–13. [PubMed: 18480811]
- Trowbridge JJ, Starczynowski DT. Innate immune pathways and inflammation in hematopoietic aging, clonal hematopoiesis, and MDS. *J Exp Med*. 2021;218(7):e20201544. [PubMed: 34129017]
- Chavakis T, Mitroulis I, Hajishengallis G. Hematopoietic progenitor cells as integrative hubs for adaptation to and fine-tuning of inflammation. *Nat Immunol*. 2019;20(7):802–11. [PubMed: 31213716]
- Pietras EM. Inflammation: a key regulator of hematopoietic stem cell fate in health and disease. *Blood*. 2017;130(15):1693–8. [PubMed: 28874349]
- Bogeska R, Mikecin AM, Kaschutnig P, Fawaz M, Büchler-Schäff M, Le D, et al. Inflammatory exposure drives long-lived impairment of hematopoietic stem cell self-renewal activity and accelerated aging. *Cell Stem Cell*. 2022;29(8):1273–84. [PubMed: 35858618]
- Hormaechea-Agulla D, Le DT, King KY. Common sources of inflammation and their impact on hematopoietic stem cell biology. *Curr Stem Cell Rep*. 2020;6:96–107.
- Kovtonyuk LV, Caiado F, Garcia-Martin S, Manz EM, Helbling P, Takizawa H, et al. IL-1 mediates microbiome-induced inflammaging of hematopoietic stem cells in mice. *Blood*. 2022;139(1):44–58. [PubMed: 34525198]
- Essers MA, Offner S, Blanco-Bose WE, Waibler Z, Kalinke U, Duchosal MA, et al. IFN $\alpha$  activates dormant haematopoietic stem cells in vivo. *Nature*. 2009;458(7240):904–8. [PubMed: 19212321]
- McCabe A, Zhang Y, Thai V, Jones M, Jordan MB, MacNamara KC. Macrophage-lineage cells negatively regulate the hematopoietic stem cell pool in response to interferon gamma at steady state and during infection. *Stem Cells*. 2015;33(7):2294–305. [PubMed: 25880153]

14. Matatall KA, Shen CC, Challen GA, King KY. Type-II interferon promotes differentiation of myeloid-biased hematopoietic stem cells. *Stem Cells*. 2014;32(11):3023–30. [PubMed: 25078851]
15. Pietras EM, Lakshminarasimhan R, Techner JM, Fong S, Flach J, Binnewies M, et al. Re-entry into quiescence protects hematopoietic stem cells from the killing effect of chronic exposure to type-I interferons. *J Exp Med*. 2014;211(2):245–62. [PubMed: 24493802]
16. Demerdash Y, Kain B, Essers MA, King KY. Yin and Yang: The dual effects of interferons on hematopoiesis. *Exp Hematol*. 2021;96:1–2. [PubMed: 33571568]
17. Strati P, Li X, Deng Q, Marques-Piubelli ML, Henderson J, Watson G, et al. Prolonged cytopenia following CD19 CAR T cell therapy is linked with bone marrow infiltration of clonally expanded IFN $\gamma$ -expressing CD8 T cells. *Cell Rep Med*. 2023;4(8):101158. [PubMed: 37586321]
18. Starczynowski DT, Kuchenbauer F, Argiropoulos B, Sung S, Morin R, Muranyi A, et al. Identification of miR-145 and miR-146a as mediators of the 5q-syndrome phenotype. *Nat Med*. 2010;16(1):49–58. [PubMed: 19898489]
19. Hartner JC, Walkley CR, Lu J, Orkin SH. ADAR1 is essential for the maintenance of hematopoiesis and suppression of interferon signaling. *Nat. Immunol*. 2009;10(1):109–15. [PubMed: 19060901]
20. Cheng X, Byrne M, Brown KD, Konopleva MY, Kornblau SM, Bennett RL, et al. PKR inhibits the DNA damage response, and is associated with poor survival in AML and accelerated leukemia in NHD13 mice. *Blood*. 2015;126(13):1585–94. [PubMed: 26202421]
21. Hu SB, Heraud-Farlow J, Sun T, Liang Z, Goradia A, Taylor S, et al. ADAR1p150 prevents MDA5 and PKR activation via distinct mechanisms to avert fatal autoinflammation. *Mol Cell*. 2023;83(21):3869–84. [PubMed: 37797622]
22. Hillmer EJ, Zhang H, Li HS, Watowich SS. STAT3 signaling in immunity. *Cytokine Growth Factor Rev*. 2016;31:1–5. [PubMed: 27185365]
23. Takeda K, Clausen BE, Kaisho T, Tsujimura T, Terada N, Forster I, et al. Enhanced Th1 activity and development of chronic enterocolitis in mice devoid of Stat3 in macrophages and neutrophils. *Immunity*. 1999;10(1):39–49. [PubMed: 10023769]
24. Chrisikos TT, Zhou Y, Kahn LM, Patel B, Denne NL, Brooks A, et al. STAT3 inhibits autocrine IFN signaling in type-I conventional dendritic cells. *J Immunol*. 2022;209(7):1286–99. [PubMed: 36038291]
25. Zhang H, Hu H, Greeley N, Jin J, Matthews AJ, Ohashi E, et al. STAT3 restrains RANK- and TLR4-mediated signalling by suppressing expression of the E2 ubiquitin-conjugating enzyme Ubc13. *Nat Commun*. 2014;5(1):5798. [PubMed: 25503582]
26. Mantel C, Messina-Graham S, Moh A, Cooper S, Hangoc G, Fu XY, et al. Mouse hematopoietic cell-targeted STAT3 deletion: stem/progenitor cell defects, mitochondrial dysfunction, ROS overproduction, and a rapid aging-like phenotype. *Blood*. 2012;120(13):2589–99. [PubMed: 22665934]
27. Melillo JA, Song L, Bhagat G, Blazquez AB, Plumlee CR, Lee C, et al. Dendritic cell (DC)-specific targeting reveals Stat3 as a negative regulator of DC function. *J Immunol*. 2010;184(5):2638–45. [PubMed: 20124100]
28. Panopoulos AD, Zhang L, Snow JW, Jones DM, Smith AM, El Kasmi KC, et al. STAT3 governs distinct pathways in emergency granulopoiesis and mature neutrophils. *Blood*. 2006;108(12):3682–90. [PubMed: 16888100]
29. Zhang H, Li HS, Hillmer EJ, Zhao Y, Chrisikos TT, Hu H, et al. Genetic rescue of lineage-balanced blood cell production reveals a crucial role for STAT3 antiinflammatory activity in hematopoiesis. *Proc Natl Acad Sci USA*. 2018;115(10):E2311–9. [PubMed: 29463696]
30. Flach J, Bakker ST, Mohrin M, Conroy PC, Pietras EM, Reynaud D, et al. Replication stress is a potent driver of functional decline in ageing haematopoietic stem cells. *Nature*. 2014;512(7513):198–202. [PubMed: 25079315]
31. Walter D, Lier A, Geiselhart A, Thalheimer FB, Huntscha S, Sobotta MC, et al. Exit from dormancy provokes DNA-damage-induced attrition in haematopoietic stem cells. *Nature*. 2015;520(7548):549–52. [PubMed: 25707806]

32. Kalogeropoulou A, Mougkogianni M, Iliadou M, Nikolopoulou E, Flordelis S, Kanellou A, et al. Intrinsic neural stem cell properties define brain hypersensitivity to genotoxic stress. *Stem Cell Rep.* 2022;17(6):1395–410.
33. Minella AC, Swanger J, Bryant E, Welcker M, Hwang H, Clurman BE. p53 and p21 form an inducible barrier that protects cells against cyclin E-cdk2 deregulation. *Curr Biol.* 2002;12(21):1817–27. [PubMed: 12419181]
34. Pant V, Quintás-Cardama A, Lozano G. The p53 pathway in hematopoiesis: lessons from mouse models, implications for humans. *Blood.* 2012;120(26):5118–27. [PubMed: 23018641]
35. Klein B, Günther C. Type-I interferon induction in cutaneous DNA damage syndromes. *Front. Immunol.* 2021;12:715723. [PubMed: 34381458]
36. Pang Q, Christianson TA, Keeble W, Koretsky T, Bagby GC. The anti-apoptotic function of Hsp70 in the interferon-inducible double-stranded RNA-dependent protein kinase-mediated death signaling pathway requires the Fanconi anemia protein, FANCC. *J Biol Chem.* 2002;277(51):49638–43. [PubMed: 12397061]
37. Piazzini M, Bavelloni A, Gallo A, Faenza I, Blalock WL. Signal transduction in ribosome biogenesis: a recipe to avoid disaster. *Int J Mol Sci.* 2019;20(11):2718. [PubMed: 31163577]
38. Kaminski JJ, Schattgen SA, Tzeng TC, Bode C, Klinman DM, Fitzgerald KA. Synthetic oligodeoxynucleotides containing suppressive TTAGGG motifs inhibit AIM2 inflammasome activation. *J Immunol.* 2013;191(7):3876–83. [PubMed: 23986531]
39. Takaoka A, Hayakawa S, Yanai H, Stoiber D, Negishi H, Kikuchi H, et al. Integration of interferon- $\alpha/\beta$  signalling to p53 responses in tumour suppression and antiviral defence. *Nature.* 2003;424(6948):516–23. [PubMed: 12872134]
40. Lee MG, Han J, Jeong SI, Her NG, Lee JH, Ha TK, et al. XAF1 directs apoptotic switch of p53 signaling through activation of HIPK2 and ZNF313. *Proc Natl Acad Sci USA.* 2014;111(43):15532–7. [PubMed: 25313037]
41. Townsend PA, Scarabelli TM, Davidson SM, Knight RA, Latchman DS, Stephanou A. STAT-1 interacts with p53 to enhance DNA damage-induced apoptosis. *J Biol Chem.* 2004;279(7):5811–20. [PubMed: 14602726]
42. Fukada T, Ohtani T, Yoshida Y, Shirogane T, Nishida K, Nakajima K, et al. STAT3 orchestrates contradictory signals in cytokine-induced G1 to S cell-cycle transition. *EMBO J.* 1998;17(22):6670–7. [PubMed: 9822610]
43. Zhang H, Nguyen-Jackson H, Panopoulos AD, Li HS, Murray PJ, Watowich SS. STAT3 controls myeloid progenitor growth during emergency granulopoiesis. *Blood.* 2010;116(14):2462–71. [PubMed: 20581311]
44. Yan D, Jobe F, Hutchison RE, Mohi G. Deletion of Stat3 enhances myeloid cell expansion and increases the severity of myeloproliferative neoplasms in Jak2V617F knock-in mice. *Leukemia.* 2015;29(10):2050–61. [PubMed: 26044284]
45. Hock H, Hamblen MJ, Rooke HM, Schindler JW, Saleque S, Fujiwara Y, et al. Gfi-1 restricts proliferation and preserves functional integrity of haematopoietic stem cells. *Nature.* 2004;431(7011):1002–7. [PubMed: 15457180]
46. Liu Y, Elf SE, Miyata Y, Sashida G, Liu Y, Huang G, et al. p53 regulates hematopoietic stem cell quiescence. *Cell Stem Cell.* 2009;4(1):37–48. [PubMed: 19128791]
47. Li X, Wilson AF, Du W, Pang Q. Cell-cycle-specific function of p53 in Fanconi anemia hematopoietic stem and progenitor cell proliferation. *Stem Cell Rep.* 2018;10(2):339–46.
48. Chen S, Yu H, Kobayashi M, Gao R, Boswell HS, Liu Y. Gain-of-function mutant p53 enhances hematopoietic stem cell self-renewal. *Blood.* 2014;124(21):260.
49. Bellodi C, Kopmar N, Ruggero D. Deregulation of oncogene-induced senescence and p53 translational control in X-linked dyskeratosis congenita. *EMBO J.* 2010;29(11):1865–76. [PubMed: 20453831]
50. Ceccaldi R, Parmar K, Mouly E, Delord M, Kim JM, Regairaz M, et al. Bone marrow failure in Fanconi anemia is triggered by an exacerbated p53/p21 DNA damage response that impairs hematopoietic stem and progenitor cells. *Cell Stem Cell.* 2012;11(1):36–49. [PubMed: 22683204]
51. Zhang Y, Lu H. Signaling to p53: ribosomal proteins find their way. *Cancer Cell.* 2009;16(5):369–77. [PubMed: 19878869]

52. Laouar Y, Welte T, Fu XY, Flavell RA. STAT3 is required for Flt3L-dependent dendritic cell differentiation. *Immunity*. 2003;19(6):903–12. [PubMed: 14670306]
53. Rouyez MC, Lestingi M, Charon M, Fichelson S, Buzyn A, Dusanter-Fourt I. IFN regulatory factor-2 cooperates with STAT1 to regulate transporter associated with antigen processing-1 promoter activity. *J Immunol*. 2005;174(7):3948–58. [PubMed: 15778351]
54. Pietras EM, Mirantes-Barbeito C, Fong S, Loeffler D, Kovtonyuk LV, Zhang S, et al. Chronic interleukin-1 exposure drives haematopoietic stem cells towards precocious myeloid differentiation at the expense of self-renewal. *Nat Cell Biol*. 2016;18(6):607–18. [PubMed: 27111842]
55. Thongon N, Ma F, Santoni A, Marchesini M, Fiorini E, Rose A, et al. Hematopoiesis under telomere attrition at the single-cell resolution. *Nat Commun*. 2021;12(1):6850. [PubMed: 34824242]
56. Masumi A, Hamaguchi I, Kuramitsu M, Mizukami T, Takizawa K, Momose H, et al. Interferon regulatory factor-2 induces megakaryopoiesis in mouse bone marrow hematopoietic cells. *FEBS Lett*. 2009;583(21):3493–500. [PubMed: 19818776]
57. Tong J, Sun T, Ma S, Zhao Y, Ju M, Gao Y, et al. Hematopoietic stem cell heterogeneity is linked to the initiation and therapeutic response of myeloproliferative neoplasms. *Cell Stem Cell*. 2021;28(3):502–13. [PubMed: 33621485]
58. Unterholzner L, Keating SE, Baran M, Horan KA, Jensen SB, Sharma S, et al. IFI16 is an innate immune sensor for intracellular DNA. *Nat Immunol*. 2010;11(11):997–1004. [PubMed: 20890285]
59. Shehata M, van Amerongen R, Zeeman AL, Girardi RR, Stingl J. The influence of tamoxifen on normal mouse mammary gland homeostasis. *Breast Cancer Res*. 2014;16(4):1–11.
60. Sánchez-Aguilera A, Méndez-Ferrer S. Regulation of hematopoietic progenitors by estrogens as a basis for new antileukemic strategies. *Mol Cell Oncol*. 2016;3(1):e1009728. [PubMed: 27308525]

**Key Points**

- STAT3 is critical for hematopoietic stem cell maintenance and function
- STAT3 inhibits DNA damage-mediated type-I interferon (IFN-I) signaling in hematopoietic stem and progenitor cells
- STAT3 prevents aberrant proliferation and p53 activation in hematopoietic progenitors by controlling autocrine IFN-I signaling

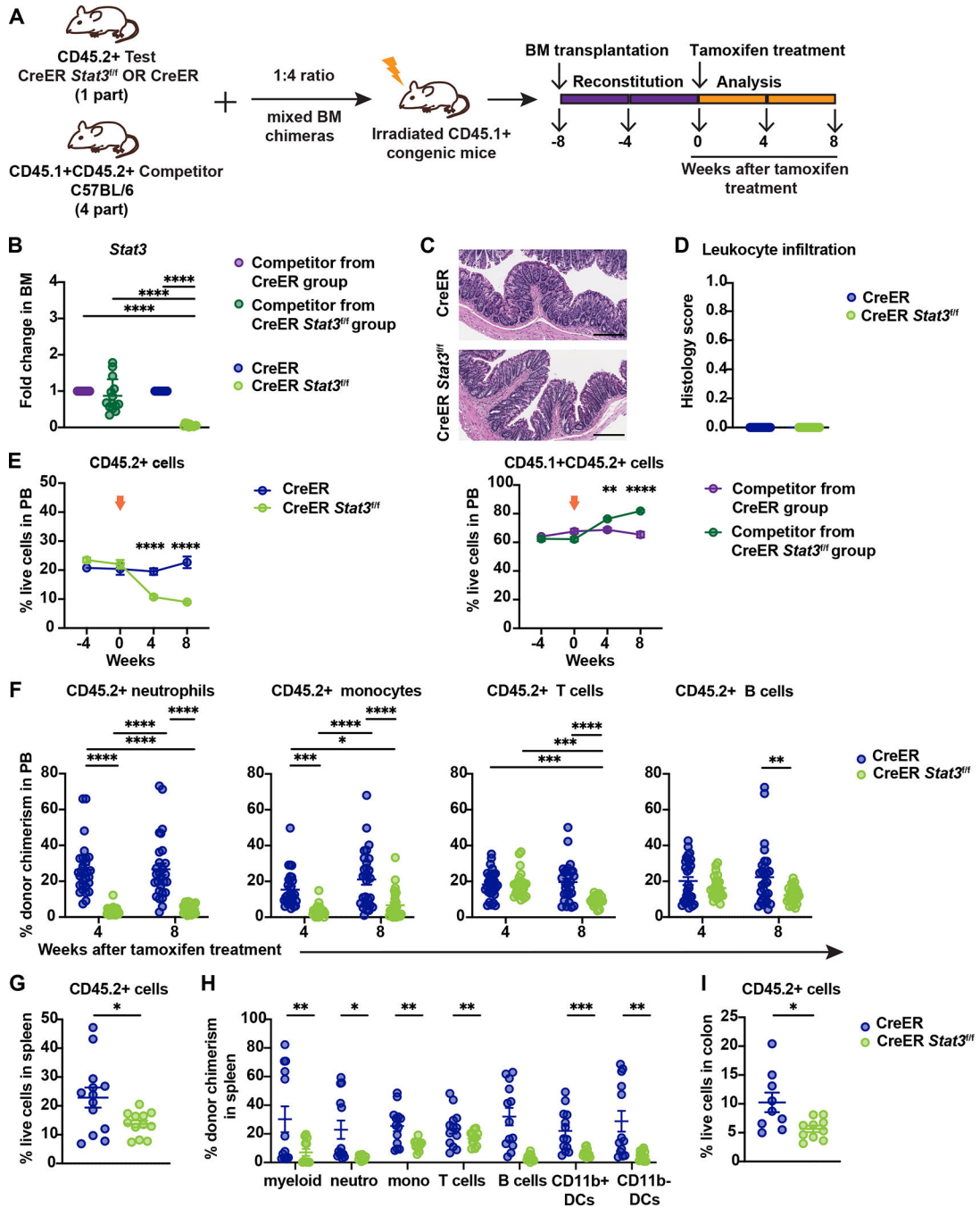


**Fig. 1. *Stat3*-deficient HSPCs show ineffective hematopoietic activity in the absence of systemic inflammation.**

(A) A schematic diagram illustrating the mixed BM chimeric model system. (B) qRT-PCR analysis of *Stat3* expression in CD45.2<sup>+</sup> test and CD45.1<sup>+</sup>CD45.2<sup>+</sup> WT competitor cells. n = 11 (CreER), n = 11 (CreER *Stat3<sup>fl/fl</sup>*), n = 14 (competitor from CreER), n = 16 (competitor from CreER *Stat3<sup>fl/fl</sup>*). (C and D) Histological assessments of colon tissues from BM chimeric mice with CreER (*Stat3*-sufficient) or CreER *Stat3<sup>fl/fl</sup>* (*Stat3*-deficient) cells 8 weeks after tamoxifen treatment. n = 13 (CreER), n = 12 (CreER *Stat3<sup>fl/fl</sup>*). (C) Representative photomicrographs of hematoxylin and eosin (H&E)-stained



colon tissue sections. Scale bars represent 200  $\mu\text{m}$ . (D) Quantification of indicated histology feature of the H&E-stained colon tissue sections. (E) Frequencies of CD45.2<sup>+</sup> test and CD45.1<sup>+</sup>CD45.2<sup>+</sup> WT competitor cells in the PB of chimeric mice at the indicated times before and after (arrows) tamoxifen treatment. n = 29 (CreER, per week), n = 27 (CreER *Stat3<sup>fl/fl</sup>*, -4 weeks), n = 25 (CreER *Stat3<sup>fl/fl</sup>*, 0 weeks), n = 26 (CreER *Stat3<sup>fl/fl</sup>*, 4 weeks), n = 26 (CreER *Stat3<sup>fl/fl</sup>*, 8 weeks), n = 29 (competitor from CreER, per week), n = 27 (competitor from CreER *Stat3<sup>fl/fl</sup>*, -4 weeks), n = 25 (competitor from CreER *Stat3<sup>fl/fl</sup>*, 0 weeks), n = 26 (competitor from CreER *Stat3<sup>fl/fl</sup>*, 4 weeks), n = 26 (competitor from CreER *Stat3<sup>fl/fl</sup>*, 8 weeks). (F) Donor chimerism of CD45.2<sup>+</sup> neutrophils (CD11b<sup>+</sup>Ly6G<sup>+</sup>Ly6C<sup>low</sup>), monocytes (CD11b<sup>+</sup>Ly6G<sup>-</sup>Ly6C<sup>high</sup>), T cells (CD3<sup>+</sup>), and B cells (B220<sup>+</sup>) in the PB of chimeric mice at the indicated times after tamoxifen treatment. Donor chimerism was determined as the percentage of the indicated population within the combined CD45.1<sup>+</sup>, CD45.2<sup>+</sup>, and CD45.1<sup>+</sup>CD45.2<sup>+</sup> cells of the same population. (G-I) Major immune cell lineages in the spleens and colons of chimeric mice 8 weeks after tamoxifen treatment. (G) Frequencies of CD45.2<sup>+</sup> cells in spleen. (H) Donor chimerism of CD45.2<sup>+</sup> myeloid cells (CD11b<sup>+</sup>), neutrophils (CD11b<sup>+</sup>Ly6G<sup>+</sup>Ly6C<sup>low</sup>), monocytes (CD11b<sup>+</sup>Ly6G<sup>-</sup>Ly6C<sup>high</sup>), T cells (CD3<sup>+</sup>), B cells (B220<sup>+</sup>), CD11b<sup>+</sup> DCs, and CD11b<sup>-</sup>DCs in spleen. n = 13 (CreER), n = 12 (CreER *Stat3<sup>fl/fl</sup>*). (I) Frequency of CD45.2<sup>+</sup> cells in colon. n = 9 (CreER), n = 10 (CreER *Stat3<sup>fl/fl</sup>*). Data in B-I are representative of 2 independent experiments. Error bars indicate means  $\pm$  SEMs. Statistical analyses were performed using two-tailed unpaired Student *t*-test (D and G-I), two-way ANOVA with the Sidak (E) or Tukey (B and F) multiple comparison test. \**P* < 0.05; \*\**P* < 0.01; \*\*\**P* < 0.001; \*\*\*\**P* < 0.0001.

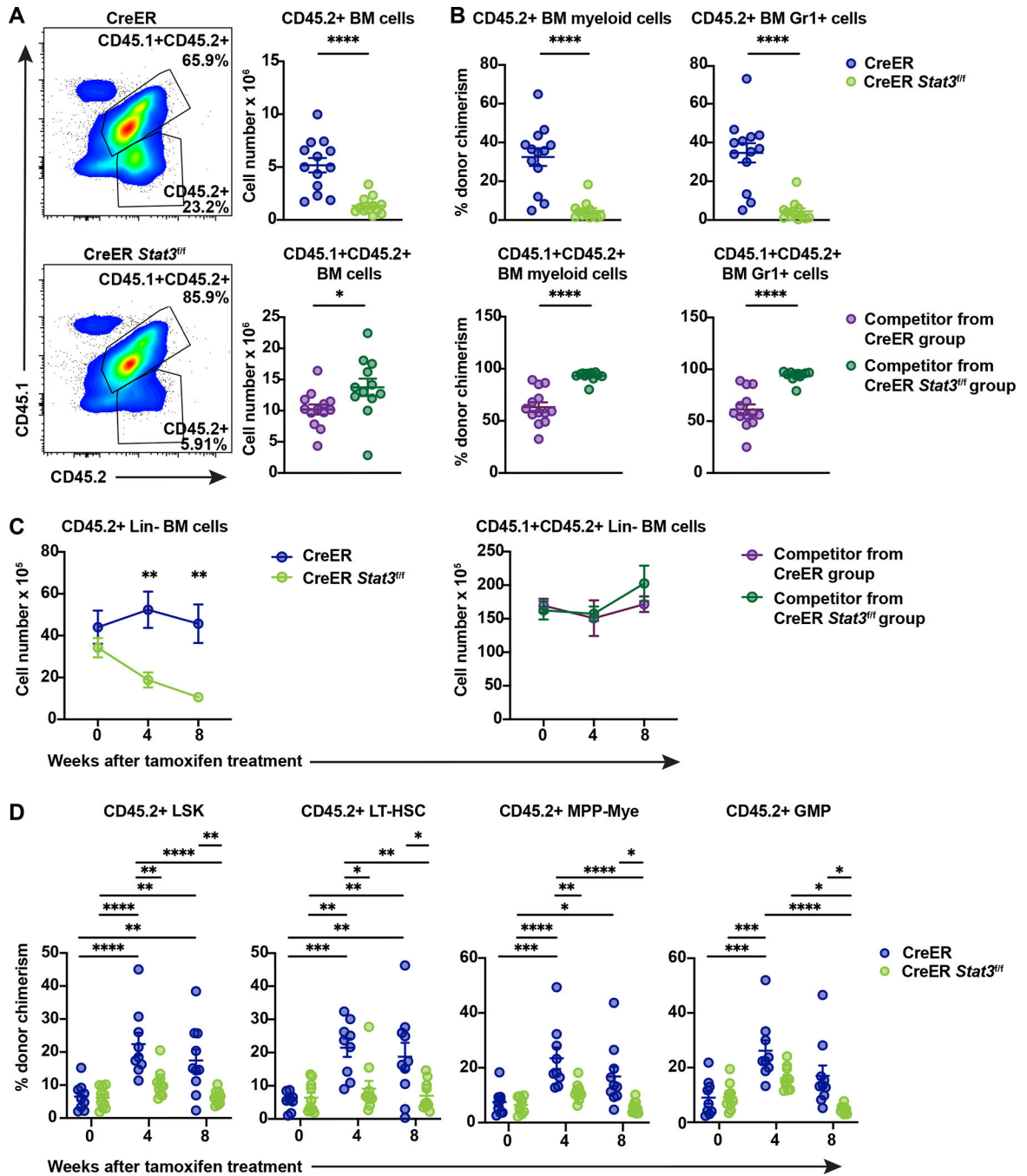


**Fig. 2. *Stat3*-deficient HSPCs show reduced competitive advantage.**

(A and B) Major immune cell lineages in total BM from chimeric mice were evaluated 8 weeks after tamoxifen treatment. (A) Representative flow cytometric plots of CD45.2<sup>+</sup> test and CD45.1<sup>+</sup>CD45.2<sup>+</sup> WT competitor cells (left) and absolute counts of these cells (right) in BM from indicated experimental groups. (B) Donor chimerism of CD45.2<sup>+</sup> test (upper panels) and CD45.1<sup>+</sup>CD45.2<sup>+</sup> WT competitor (lower panels) myeloid (CD11b<sup>+</sup>) and Gr1<sup>+</sup> cells in BM from indicated experimental groups. n = 13 (CreER), n = 12 (CreER *Stat3*<sup>fl/fl</sup>), n = 13 (competitor from CreER), n = 12 (competitor from CreER *Stat3*<sup>fl/fl</sup>). (C

and D) Lin<sup>-</sup> cells from BM chimeric mice were evaluated at the indicated times after *Stat3* deletion. n = 9 (CreER, 0 weeks), n = 9 (CreER, 4 weeks), n = 10 (CreER, 8 weeks), n = 10 (CreER *Stat3<sup>fl/fl</sup>*) for all timepoints. (C) Absolute numbers of Lin<sup>-</sup>CD45.2<sup>+</sup> test and CD45.1<sup>+</sup>CD45.2<sup>+</sup> WT competitor cells in BM. (D) Donor chimerism of CD45.2<sup>+</sup> LSK (Lin<sup>-</sup>ckit<sup>+</sup>Sca1<sup>+</sup>), LT-HSC (Lin<sup>-</sup>ckit<sup>+</sup>Sca1<sup>+</sup>CD135<sup>-</sup>CD34<sup>-</sup>CD48<sup>-</sup>CD150<sup>+</sup>), MPP-My (Lin<sup>-</sup>ckit<sup>+</sup>Sca1<sup>+</sup>CD135<sup>-</sup>CD48<sup>+</sup>CD150<sup>-</sup>), and GMP (Lin<sup>-</sup>CD127<sup>-</sup>ckit<sup>+</sup>Sca1<sup>-</sup>CD16/32<sup>+</sup>CD34<sup>+</sup>) populations in BM. Data are representative of 2 independent experiments. Error bars indicate means ± SEMs. Statistical analyses were performed using a two-tailed unpaired Student *t*-test (A and B) or with two-way ANOVA with the Sidak (C) or Tukey (D) multiple comparison test. \**P* < 0.05; \*\**P* < 0.01; \*\*\**P* < 0.001; \*\*\*\**P* < 0.0001.

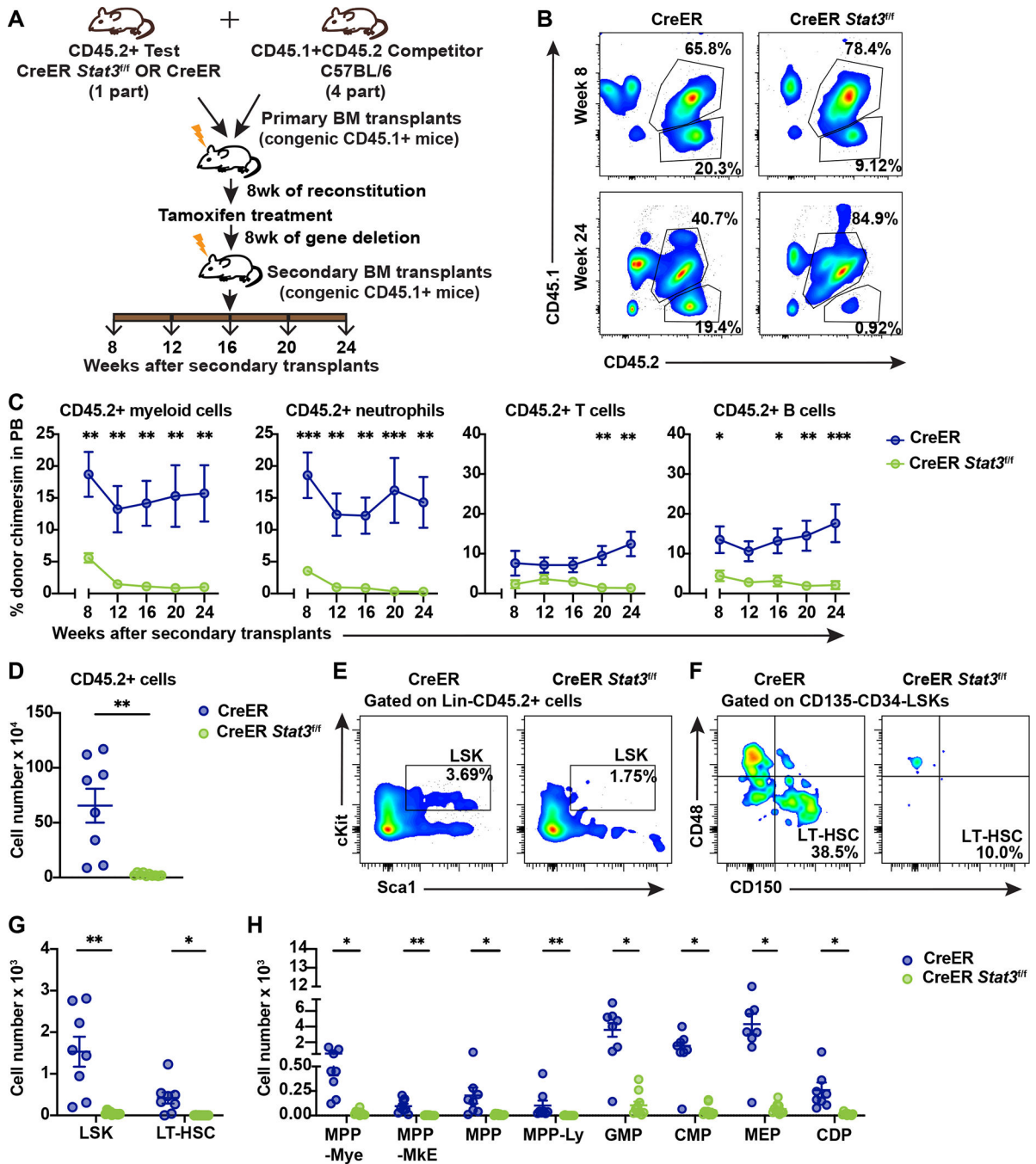


**Fig. 3. STAT3 is required to maintain HSC function.**

(A) A schematic diagram showing the experimental design for the secondary BM transplantation assays. (B) Representative flow cytometric plots showing proportions of CD45.2<sup>+</sup> test and CD45.1<sup>+</sup>CD45.2<sup>+</sup> WT competitor cells in the PB of chimeric mice with CreER (*Stat3*-sufficient) or CreER *Stat3*<sup>fl/fl</sup> (*Stat3*-deficient) BM after secondary BM transplantation. (C) Donor chimerism of CD45.2<sup>+</sup> myeloid cells (CD11b<sup>+</sup>), neutrophils (CD11b<sup>+</sup>Ly6G<sup>+</sup>Ly6C<sup>low</sup>), T cells (CD3<sup>+</sup>), and B cells (B220<sup>+</sup>) in PB at the indicated times after secondary BM transplantation. n = 10 (CreER, 8 weeks), n = 9 (CreER,

12 weeks), n = 10 (CreER, 16 weeks), n = 8 (CreER, 20 weeks), n = 7 (CreER, 24 weeks), n = 11 (CreER *Stat3<sup>fl/fl</sup>*, 8 weeks), n = 11 (CreER *Stat3<sup>fl/fl</sup>*, 12 weeks), n = 11 (CreER *Stat3<sup>fl/fl</sup>*, 16 weeks), n = 11 (CreER *Stat3<sup>fl/fl</sup>*, 20 weeks), n = 10 (CreER *Stat3<sup>fl/fl</sup>*, 24 weeks). (D-H) BM progenitors were evaluated 24 weeks after secondary BM transplantation. (D) Absolute numbers of CD45.2<sup>+</sup> cells in BM. (E) Representative flow cytometric plots showing proportions of CD45.2<sup>+</sup> LSKs (Lin<sup>-</sup>ckit<sup>+</sup>Sca1<sup>+</sup>) in the indicated mice. (F) Representative flow cytometric plots showing proportions of CD45.2<sup>+</sup> LSKs LT-HSCs (Lin<sup>-</sup>ckit<sup>+</sup>Sca1<sup>+</sup>CD135<sup>-</sup>CD34<sup>-</sup>CD48<sup>-</sup>CD150<sup>+</sup>) in the indicated mice. (G) Absolute numbers of CD45.2<sup>+</sup> LSKs and LT-HSCs in the indicated mice. (H) Absolute numbers of CD45.2<sup>+</sup> MPP-My (Lin<sup>-</sup>ckit<sup>+</sup>Sca1<sup>+</sup>CD135<sup>-</sup>CD48<sup>+</sup>CD150<sup>-</sup>), MPP-MkE (Lin<sup>-</sup>ckit<sup>+</sup>Sca1<sup>+</sup>CD135<sup>-</sup>CD48<sup>+</sup>CD150<sup>+</sup>), MPPs (Lin<sup>-</sup>ckit<sup>+</sup>Sca1<sup>+</sup>CD135<sup>-</sup>CD48<sup>-</sup>CD150<sup>-</sup>), MPP-Ly (Lin<sup>-</sup>ckit<sup>+</sup>Sca1<sup>+</sup>CD135<sup>+</sup>CD150<sup>-</sup>), GMPs (Lin<sup>-</sup>CD127<sup>-</sup>ckit<sup>+</sup>Sca1<sup>-</sup>CD16/32<sup>+</sup>CD34<sup>+</sup>), CMPs (Lin<sup>-</sup>CD127<sup>-</sup>ckit<sup>+</sup>Sca1<sup>-</sup>CD16/32<sup>-</sup>CD34<sup>+</sup>), MEPs (Lin<sup>-</sup>CD127<sup>-</sup>ckit<sup>+</sup>Sca1<sup>-</sup>CD16/32<sup>-</sup>CD34<sup>-</sup>), and CDPs (Lin<sup>-</sup>CD127<sup>-</sup>ckit<sup>low</sup>CD115<sup>+</sup>CD135<sup>+</sup>) in the indicated mice. n = 8 (CreER), n = 10 (CreER *Stat3<sup>fl/fl</sup>*). Data in B-H are representative of 2 independent experiments. Error bars indicate mean ± SEMs. Statistical analyses were performed using two-way ANOVA with the Sidak (C) or Tukey multiple comparison (G) test or using a two-tailed unpaired Student *t*-test (D and H). \**P* < 0.05; \*\**P* < 0.01, \*\*\**P* < 0.001.

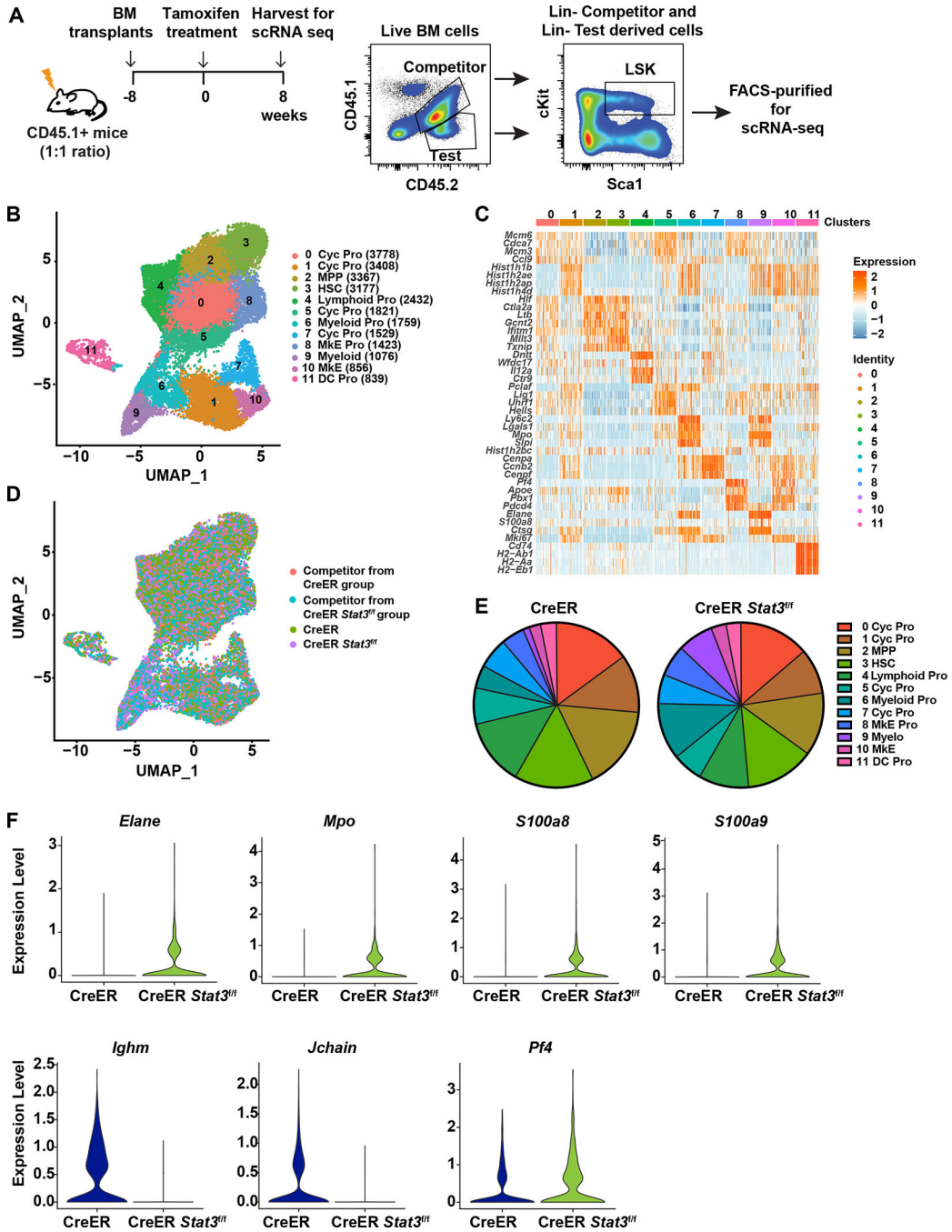


**Fig. 4. *Stat3*-deficient LSKs have a unique transcriptional profile and myeloid-biased gene expression.**

(A) A schematic diagram showing the experimental design for using 1:1 ratio of CD45.2<sup>+</sup> test and CD45.1<sup>+</sup>CD45.2<sup>+</sup> WT competitor cells to generate BM chimeric mice with sufficient LSKs for scRNA-seq analysis. (B) UMAP plot showing 12 clusters in the integrated LSK compartment, including 12174 CD45.2<sup>+</sup> CreER LSKs and 9822 CD45.1<sup>+</sup>CD45.2<sup>+</sup> WT competitor LSKs from CreER (*Stat3*-sufficient) BM chimeric mice and 8864 CD45.2<sup>+</sup> CreER *Stat3*<sup>fl/fl</sup> LSKs and 11322 CD45.1<sup>+</sup>CD45.2<sup>+</sup> WT competitor LSKs from CreER *Stat3*<sup>fl/fl</sup> (*Stat3*-deficient) BM chimeric mice. Results were pooled to

generate a merged dataset.  $n = 15$  mice per group. Different colors represent distinct clusters (or transcriptional states) based on differential gene expression signatures. Each dot represents a single cell. Numbers in parentheses beside each cluster indicate cell numbers in that cluster. (C) Heatmap displaying cluster-defining stem cell- and lineage-specific gene expression. (D) UMAP plot showing the distribution of the 4 experimental groups in the integrated LSK compartment. Different colors represent different experimental groups. (E) Proportions of individual clusters represented as percentages of the total cells in each experimental group. (F) Violin plots showing the expression of myeloid lineage-specific genes (*Mpo*, *Elane*, *S100a8*, and *S100a9*), lymphoid-specific genes (*Ighm* and *Jchain*) and megakaryocyte-specific gene (*Pf4*) in cluster 3 (HSCs) from CreER LSKs and CreER *Stat3<sup>f/f</sup>* LSKs.

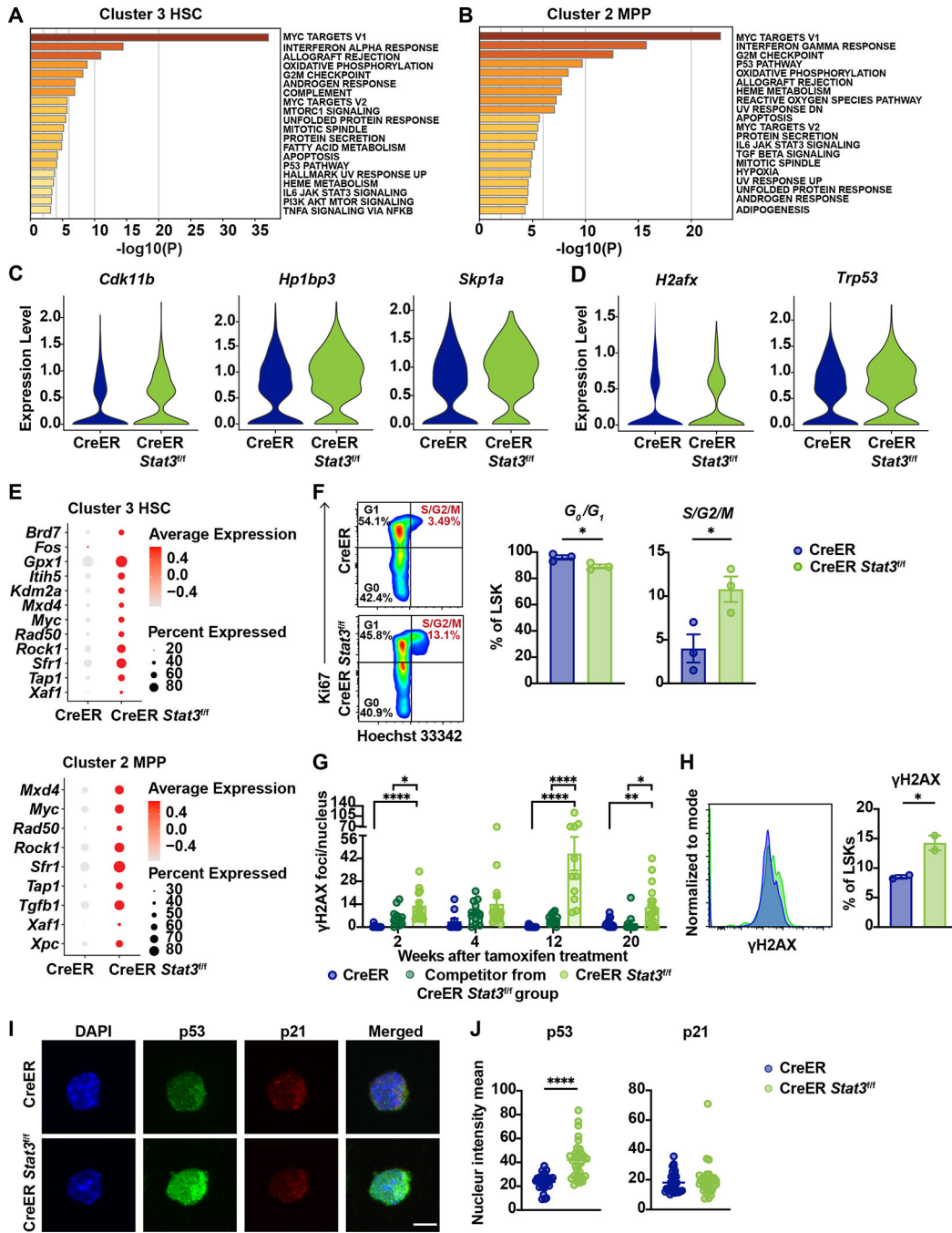


**Fig. 5. Cell cycle deregulation, p53 activation, and DNA damage in *Stat3*-deficient LSKs.** (A-E) LSKs were purified from BM chimeric mice 8 weeks after tamoxifen treatment and processed for scRNA-seq analysis as indicated in Figure 4. (A) Metascape pathway enrichment analysis of differentially expressed genes in cluster 3 (HSCs). The top 20 hallmark gene sets are shown for the comparison between CreER *Stat3*<sup>f/f</sup> (*Stat3*-deficient) HSCs and CreER (*Stat3*-sufficient) HSCs. (B) Metascape pathway enrichment analysis of differentially expressed genes in cluster 2 (MPPs). The top 20 hallmark gene sets are shown for the comparison between CreER *Stat3*<sup>f/f</sup> (*Stat3*-deficient) MPPs and CreER



(*Stat3*-sufficient) MPPs. (C) Violin plots showing the expression levels of genes associated with cell cycle regulation in cluster 3 (HSCs) from the indicated experimental groups. (D) Violin plots showing the expression levels of genes associated with stress response in cluster 3 (HSCs) from the indicated experimental groups. (E) Dot plot showing differentially expressed genes associated with p53 transcriptional response in cluster 3 (HSCs) (top) and in cluster 2 (MPPs) (bottom) from the indicated experimental groups. (F) LSKs from CreER or CreER *Stat3<sup>f/f</sup>* mice were FACS purified and cultured for 3 days with stem cell factor (SCF) and 4-hydroxytamoxifen to induce *Stat3* deletion in vitro. n = 3 for both groups. The frequency of LSKs in G0, G1, and S/G2/M phases was assessed by intracellular Ki-67 and Hoechst 33342 staining. Representative (left) and cumulative (right) results shown. (G) Quantification of  $\gamma$ H2AX foci. LSKs were purified from BM chimeric mice of the indicated experimental groups at 2, 4, 12, or 20 weeks following tamoxifen treatment in vivo, as indicated. n = 6 (CreER), n = 4 (Competitor from CreER *Stat3<sup>f/f</sup>*), n = 5 (CreER *Stat3<sup>f/f</sup>*) for all timepoints. LSKs were stained with DAPI and with anti- $\gamma$ H2AX antibody prior to confocal imaging and analysis with Imaris software. Each data point represents the  $\gamma$ H2AX foci count per nucleus for 1 field of view (n = at least 10 fields of view). (H-J) LSKs were cultured in vitro with SCF and 4-hydroxytamoxifen as indicated in (F). (H) Representative (left) and cumulative (right) results showing  $\gamma$ H2AX expression in LSKs following culture in vitro as indicated in (F). n = 2 for both groups. (I) Representative immunofluorescence images showing p53 (green), p21 (red) and (4',6-diamidino-2-phenylindole) DAPI/nucleus (blue) in the indicated experimental groups. (J) Quantification of mean fluorescence intensity of nuclear p53 (left) and p21 (right) in LSKs from the indicated experimental groups. n = 10 (CreER), n = 11 (CreER *Stat3<sup>f/f</sup>*). Each data point represents mean fluorescence intensity of p53 or p21 per nucleus in 1 field of view (n = at least 10 fields of view). In F, G, H and J, error bars indicate means  $\pm$  SEMs. Statistical analyses were performed using two-tailed unpaired Student *t*-test (F, H and J) or one-way ANOVA (G) with the Tukey multiple comparison test. \**P* < 0.05; \*\**P* < 0.01; \*\*\*\**P* < 0.0001.

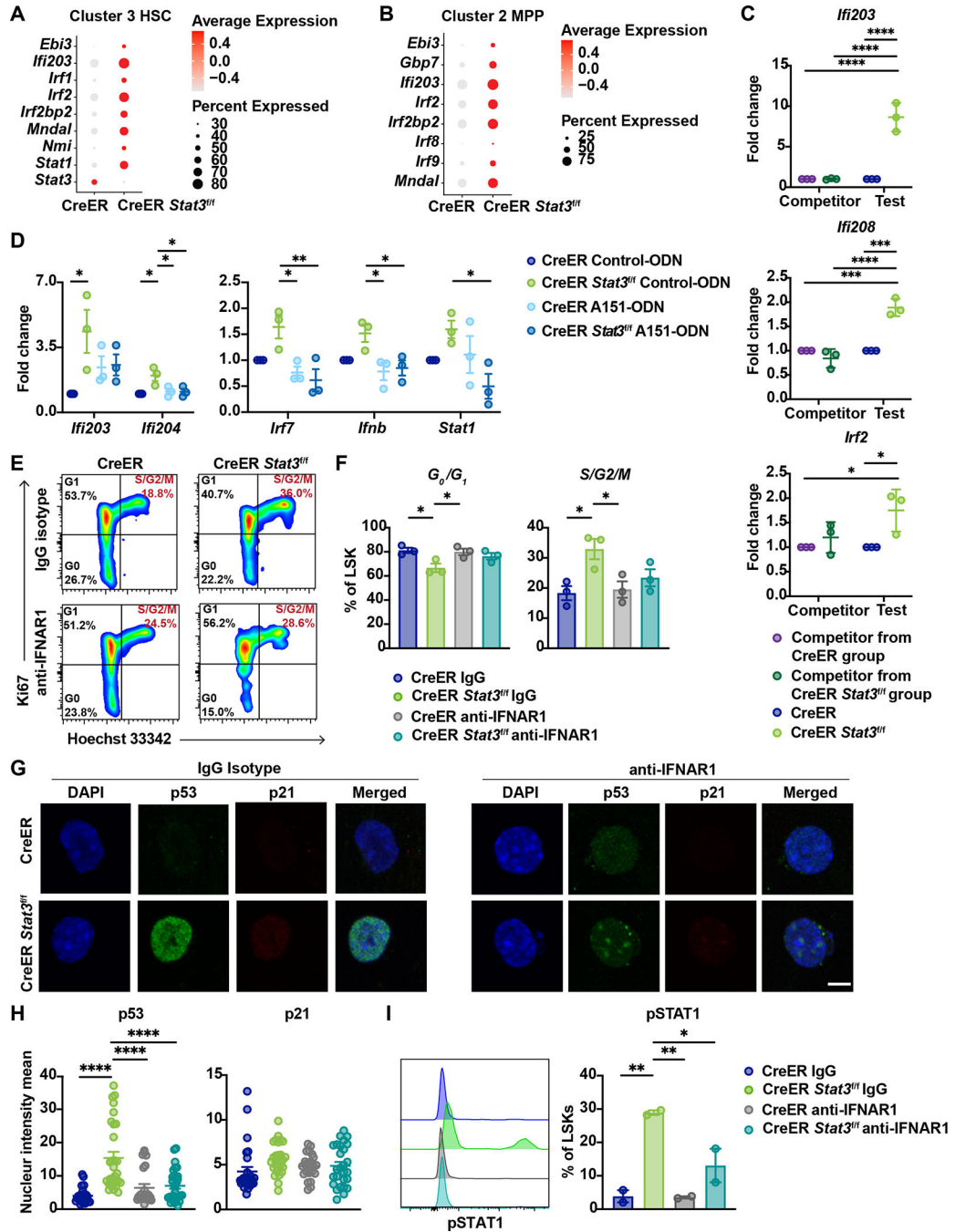


**Fig. 6. STAT3 prevents p53 activation in LSKs by inhibiting autocrine IFN signaling.** (A and B) LSKs were purified from BM chimeric mice 8 weeks after tamoxifen treatment and processed for scRNA-seq analysis as indicated in Figure 4. (A) Dot plot showing differentially expressed genes associated with the IFN transcriptional response in cluster 3 (HSCs) from chimeric mice with CreER (*Stat3*-sufficient) or CreER *Stat3*<sup>fl/fl</sup> (*Stat3*-deficient) BM. (B) Dot plot showing differentially expressed genes associated with the IFN transcriptional response in cluster 2 (MPPs) from the indicated experimental groups. (C) qRT-PCR analysis of IFN-inducible and -regulatory genes in total CD45.2<sup>+</sup> (CreER

or CreER *Stat3<sup>fl/fl</sup>* and CD45.1<sup>+</sup> CD45.2<sup>+</sup> WT competitor BM cells from BM chimeric mice. n = 3 for all groups. (D-I) LSKs from CreER and CreER *Stat3<sup>fl/fl</sup>* mice were FACS purified and cultured for 3 days in vitro with SCF and 4-hydroxytamoxifen as indicated in Figure 5. Cells were incubated with A151-ODN, Control-ODN, IFNAR1 antibody or IgG isotype, as indicated. (D) qRT-PCR analysis of DNA sensors, IFN-Is and IFN-responsive genes. n = 3 for all groups. (E and F) The frequency of LSKs in G0, G1, and S/G2/M phases was assessed by intracellular Ki-67 and Hoechst 33342 staining. Representative (left) and cumulative (right) results shown. n = 3 for all groups. (G) Representative immunofluorescence images showing p53 (green), p21 (red) and (4',6-diamidino-2-phenylindole) DAPI/nucleus (blue) in LSKs from the indicated experimental groups. Magnification 63x. Scale bars represent 30 mm. (H) Quantification of mean fluorescence intensity of nuclear p53 (left) and p21 (right) in LSKs from the indicated experimental groups. n = 10 (CreER), n = 11 (CreER *Stat3<sup>fl/fl</sup>*) for both treatments. Each data point represents the mean fluorescence intensity of p53 or p21 per nucleus in 1 field of view (n = at least 10 fields of view). (I) Representative (left) and cumulative (right) results showing STAT1 phosphorylation in LSKs from the indicated experimental groups. n = 2 for all groups. Statistical analyses were performed using two-way ANOVA (C) or one-way ANOVA (D, F, H and I) with the Tukey multiple comparison test. \**P* < 0.05; \*\**P* < 0.01; \*\*\**P* < 0.001; \*\*\*\**P* < 0.0001.